

Design of an Off-Grid Hybrid Power Generation System for a Telecommunication Base-Transceiver Station: A Case Study of Cell Site at Oke-Imobi, Nigeria

Patrick O. Olabisi^{1*}, Olusola Ajayi¹

¹ Department of Electrical, Electronic & Telecommunication Engineering,
College of Engineering, Bells University of Technology, Ota, NIGERIA

*Corresponding Author: niyiolabisi@gmail.com
DOI: <https://doi.org/10.30880/jeva.2024.06.01.004>

Article Info

Received: 17 February 2025
Accepted: 21 May 2025
Available online: 30 June 2025

Keywords

Hybrid power supply, energy resources, basic infrastructure, geographical location, cell sites, off-grid power

Abstract

Hybrid of energy resources has proved to be an innovative means of providing off-grid power to infrastructures in remote locations where there is limited access to the national power supply grid. Adopting a mix of renewable energy resources with battery backup, and gas generator, to determine the optimum mix of the energy resources to meet particular load demands is a major challenge. Load profile for the case cell site was used as input to the simulation software, HOMER (evaluation version), to simulate the mix of energy resources to meet optimum power supply requirement. For cost effective power solution, the optimum period of 4–6 hours per day and a converter of 3 kW were used to obtain the following results for various mix: use of solar, wind and gas generator with 78.4 hours Autonomy produced 6,319 kWh/yr, in excess by 1694 kWh/yr (26.8%), Zero Unmet load and Capacity Shortage; use of solar and gas generator with 85.3 hours Autonomy produced 6,126 kWh/yr., in excess by 1526 kWh/yr (24.8%), with Zero Unmet load and Capacity Shortage; use of wind and gas generator with 177 hours Autonomy produced 5043 kWh/yr in excess by 198 kWh/yr (3.92%), Zero Unmet load and Zero Capacity Shortage; and, the use of solar and wind with 19.7 hours Autonomy produced 4,509 kWh/yr in excess by 632 kWh/yr, (14%), Unmet load of 621 kWh/yr and Capacity Shortage of 811 kWh/yr. Therefore, for the study area, the use of wind and gas generator produced the optimal supply of highest autonomy and minimal excess power with unmet load and zero capacity shortage.

1. Introduction

Inadequacies of electrical power infrastructures have created serious limitations to the supply of adequate electricity to power different applications and facilities like the telecommunication Base Transceiver Stations (BTS) installed particularly in remote areas. Limitations in the provision of robust connection of telecommunication facilities pose major issues to the growth of broadband connectivity in developing countries like Nigeria. Issues of power and connectivity are among major challenges that may disenfranchise 5G deployment in such countries [1], [2], [3], [4]. With the Nigerian approximated installed power capacity of about 13,500 Megawatts (MW), only about 8,000 MW of it is injected into the transmission grid with about 5,000 MW or less available for distribution to over 200 million people. This confirms the existence of major constraints in the country's electrical power network [5].

Providing power for major and basic infrastructures in Nigeria has been a major challenge seriously affecting the growth of the country's economy. For the size of telecommunication infrastructure, it is noted that the Nigeria

telecommunication market is the largest in Africa with over 20,000-50,000 installed Telecommunication Cell Sites (TCS) scattered over the nation's geographical area [6].

However, only an average of 5 to 12 hours of power or none at all at some locations is supplied per day to the TCSs from the national grid. With this, the Mobile Network Operators (MNOs) and site operators are forced to deploy diesel generators to provide stable power to telecom equipment from the onset in order to ensure that numerous subscribers all over the country are satisfied [7]. The reliance on diesel generators as primary source of power is a big problem that cannot be over-estimated. Apart from the high operational cost, the use of diesel to fuel power generators emit harmful gases of methane (CH_4), nitrogen oxides (NO_x), fluorinated gases and carbon monoxide (CO) into the atmosphere with the resultant effects on the climate and the human health [8].

With the need to bring telecommunication services close to the people irrespective of their geographical location, income, political affiliation, age, gender, or any other discriminatory factors [9], no nation can develop and sustain its development without its population and key infrastructures having access to adequate energy [5], [10]. Energy is critical for socioeconomic growth and poverty alleviation [11]; hence access to clean efficient energy is a struggle for the African continent where typically, about 60-70 % of the Nigeria's population does not have access to constant electricity supply [12], [13].

This study discussed the design of an off-grid hybrid power generation system that combined renewable energy sources of solar and wind with the diesel generator to provide off-grid power to the TCS. This is done from the technical, economic, and environmental viewpoints. The aim is to analyse how these energy sources could be used to optimally meet the energy demand of TCSs in rural communities like the one at the Oke-Imobi, a remote community in the Northern side of Ogun State in Nigeria.

Renewable energy sources like hydro, solar, wind, biomass and so on, are off-grid energy systems that promise to provide solution to the problem of lack or shortage of energy supply to infrastructures particularly at remote locations not connected to the national power grid across the country [14]. This study is focused on the design, planning and implementation of optimal off-grid hybrid power generation for remote telecom BTS's. This system combined diesel-powered generators with renewable energy sources of solar and wind along with backup battery banks as storage system to ensure optimal availability, reliability and security of power supply, as shown in Fig. 1.

1.1 Photovoltaic (PV) System Parameters

In standard photovoltaic systems, basic parameters for describing the performance of solar PV systems are discussed as follows [15], [16], [17]:

- i. Open-circuit voltage, (V_{oc}), is given as the peak Direct Current (DC) voltage on the Current-Voltage (I-V) characteristics curve. It reflects the operating voltage when there is no load, when the current and power values are zero in an open-circuit (no load) state. It is unaffected by the size of the solar panel but decreases in value as the temperature of the panel rises.
- ii. Short-circuit current, (I_{sc}), is the peak Direct Current on the characteristic curve obtained in a short-circuit state, with the values of the voltage and power being negative. It is proportional to the solar irradiance. As a result, a site with strong solar irradiation periods would be appropriate for solar-powered energy systems.
- iii. Maximum power point current, (I_{mpp}), is the magnitude of current when the solar panel is operating at the maximum power point and the value of the voltage is equivalent to V_{mpp} . For some solar cells, the I_{mpp} is about 90% of the I_{sc} .
- iv. Maximum power point voltage, (V_{mpp}), is the voltage of the solar panel when the output power is at its peak. It is typically 0.7-0.8 of V_{oc} , and it is the voltage equivalence of the peak power current, I_{mpp} .
- v. Maximum power point, (P_{mpp}), is the peak power obtained from the output voltage and current of the solar panel as indicated on the I-V characteristics curve. With the use of a charge controller, the maximum power point tracking (MPPT) ensures the PV modules operate at the maximum power point.
- vi. Series resistance, (R_s), is the minimum resistance value obtained from the diode model required for optimising the efficiency of conversion by the solar panel.
- vii. Shunt resistance, (R_{sh}), is the maximum resistance value required for optimising the efficiency of conversion by the solar panel.
- viii. The Balance of System (BOS) of PV systems describes all components other than the PV. These include inverters, batteries, solar charge controllers, power conditioners, switches, wiring, and combiner box. Figure 1 shows the hybrid power system architecture.

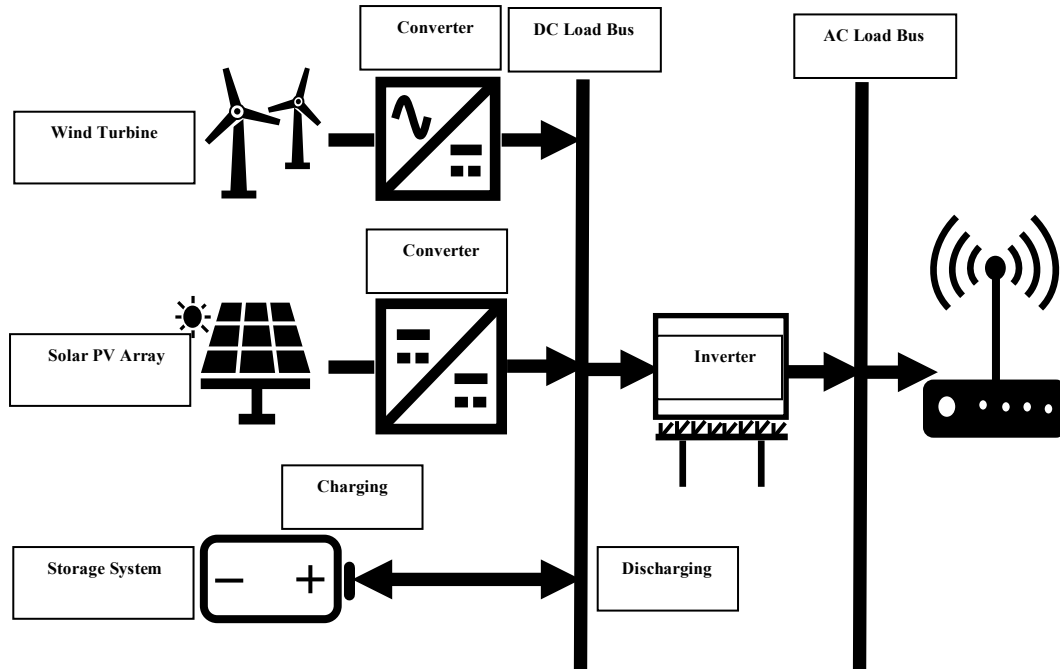


Fig. 1 Typical hybrid power system architecture [27]

1.2 Wind Turbine Power Systems

A wind turbine is specially built to convert wind energy into mechanical energy which is further converted by the wind generator into electrical energy to power a load. There are varieties of the design of wind turbine which include the most well-known Flat Hub Turbine (FHT), the Horizontal Axis Wind Turbine (HAWT), and the less efficient Vertical Axis Wind Turbine (VAWT) [18], [19].

The turbine framework uses a fixed speed rotor with three variable pitch cutting edges that are naturally adjusted to maintain a constant turn speed regardless of wind speed. The large rotor edges are necessary for capturing the most air stream resulting in high tip speeds. Due to high disturbance and commotion levels, tip speeds are limited, leading to low turn rates of between 10 and 20 revolution per minute (RPM) for large wind turbines. The rotor drives a simultaneous generator via a stuff box, and the complete module is contained in a nacelle above a pinnacle, requiring massive building work including many cubic meters of built-up concrete. A gearbox is utilized to achieve a speed enough to drive the generator to its designed constant operating speed. The construction of the foundation work comes with reinforcement that can support and ensure that the wind turbine will withstand all wind turbulence that may arise over a long period of time [18], [19].

The force P generated in the wind speed is the force exerted on the blade and it is given by Equation (1) [20]:

$$P = \frac{CA\rho V^2}{2} \quad (1)$$

Where, C is a power efficiency factor that depends on the machine design and geographic location of wind front blocked by the cleared side of the rotor edges, A is the area of the wind blade, ρ is the air gap at about 1.225 kg/m^3 density, and V is the wind speed.

1.3 Battery as Storage

Batteries are energy storage devices that serve as energy source to provide power to the TCS equipment whenever supply from the main energy sources is low and cannot effectively power the load or during power supply maintenance. The battery system powers the load till the renewable energy sources are fully restored. Types of batteries used in this case include the Lead Acid (LA) battery which, due to its high cell voltage and lower cost, is mostly deployed for power backup in power plants and substations [21]. Other specialised batteries which could also be used are the Vanadium Redox Flow (VRF) battery [22], [23], high-energy and prelithiation-strategies Lithium-ions battery [24], [25], and the Zero Emission Batteries Research Activity (ZEBRA) battery [26].

| Nomenclatures | | | |
|-----------------|---|---------------|---|
| BOS | Balance of System | I_{sc} | Charge controller short-circuit current |
| BTS | Base Transceiver Station | $In v_{size}$ | Capacity of inverter (kVA) |
| CH ₄ | Methane | L_i | Inductive load (kW) |
| CO | Carbon monoxide | L_{out} | Other loads (kW) |
| COE | Cost of Electricity | I_{mpp} | Maximum power point current |
| HAWT | Horizontal Axis Wind Turbine | I_{sc} | Short-circuit current |
| HOMER | Hybrid Optimization of Multiple Energy Resource | NO_x | Nitrogen oxides |
| GHI | Global Horizontal Irradiance | N_s | Numbers of cells connected in series |
| KWh | kilo Watt hour | P_{mpp} | Maximum power point |
| LA | Lead Acid | R_s | Series resistance |
| MNO | Mobile Network Operators | R_{sh} | Shunt resistance |
| MW | Megawatts | R_p | Equivalent parallel resistance |
| NPC | Net Present Cost | R_s | Equivalent series resistance |
| TCS | Telecommunication Cell Sites | V_{mpp} | Maximum power point voltage |
| VAWT | Vertical Axis Wind Turbine | V_{oc} | Open-circuit voltage |
| VRB | Vanadium Redox Battery | P_r | Wind turbine's rated output power |
| ZEBRA | Zero Emission Batteries Research Activity | v_w | Actual wind speed |
| C_{BAh} | Battery energy storage capacity | v_{in} | Wind turbine's cut-in speed |
| $C_{ann,tot}$ | Total annualized cost of a system | v_r | Turbine's rated speed |
| CRF | Capital recovery factor | v_{out} | Turbine's cut-off/out speed |
| CR_{size} | Capacity of the solar charge controller | V_t | Thermal voltage of PV modules |
| I_{pv} | Photovoltaic current | α | Short-circuit temperature coefficient |
| I_0 | Saturation current | η_{BAh} | Round trip battery efficiency |

2. Methods and Materials

Over time, studies in this area have focused on techno-environmental and techno-economic analysis of power supply optimization [28]. However, this study focused on the conduct of technical, environmental, and economical analysis, based on addition of solar PV and wind renewable energy sources into existing off-grid diesel generator power supply. The load profile of a remote TCS was modeled and simulated, and the analyses of the off-grid power sources were carried out. The Hybrid Optimization of Multiple Energy Resources (HOMER) pro-version 3.14.5 application program was utilised to decide the spans of various energy-producing frameworks in the energy blend required to effectively power the TCS. The HOMER version used was the evaluation edition with "For Evaluation Use" stamped on results obtained by the software.

Electric load of the TCS comprises of radio, antennas, microwave, BTS auxiliary power, air conditioner and lighting. The technical data of these load parameters were used as inputs to the Hybrid Optimization of Multiple Energy Resource (HOMER) simulation tool. HOMER was used to optimise, simulate, and give sensitivity analysis to create the daily load profile and energy supply requirement for a TCS at Oke-Imobi with location at Longitude & Latitude of 6.65° and 4.19694° and average temperature of 24°C and 32°C respectively were adopted. Oke-Imobi is a developing rural area with small scale industries like wood sawmills, agriculture processing, small-scale poultry yards, and about two elementary Community schools.

2.1 Energy Resource Data for Solar at Oke-Imobi in Ogun State, Nigeria

To generate solar data, it is required to know the temperature, Global Horizontal Irradiance (GHI), and Clearness index of the area as follows [29]

Fig. 2 shows the load demand of the BTS devices with the energy consumption of the devices put in percentage range is shown in Fig. 3. The energy resource data was downloaded from the power solar database of the National Aeronautics and Space Administration (NASA) website as point download for the Oke-Imobi community [30] based on the given longitude and latitude dimensions. The values of the energy resources parameters for Oke-Imobi are given in Table 1. The data is monthly solar GHI (kWh/m²), Clearness Index, Average Temperature (°C) and Average Wind Speed (m/s).

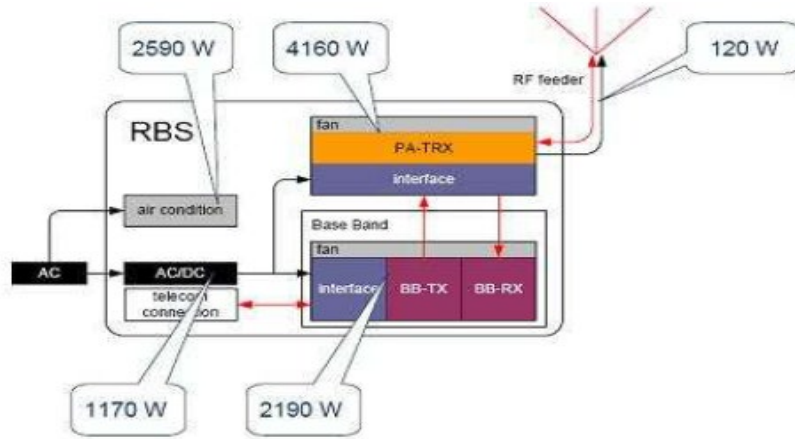


Fig. 2 Required power for devices of a typical radio base station [32]

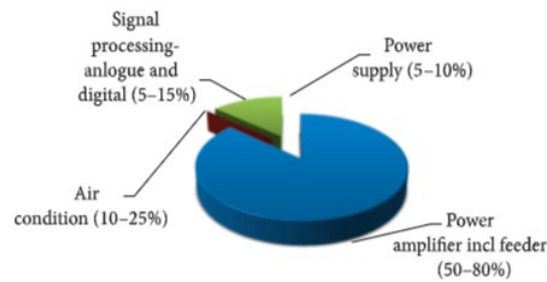


Fig. 3 Energy consumption of the components of a BTS [33]

Table 1 Solar and wind data for Oke-Imobi (HOMER optimisation software)

| Month | Daily Radiation (kWh/m ² /d) | Clearness Index | Aver. Temp. (°C) | Aver. Wind Speed (m/s) |
|-----------|---|-----------------|------------------|------------------------|
| January | 5.28 | 0.529 | 25.26 | 2.41 |
| February | 5.49 | 0.504 | 26.49 | 2.74 |
| March | 5.46 | 0.586 | 26.85 | 2.97 |
| April | 5.21 | 0.544 | 26.64 | 2.97 |
| May | 4.76 | 0.519 | 26.16 | 2.75 |
| June | 4.04 | 0.473 | 25.27 | 2.99 |
| July | 3.95 | 0.412 | 24.42 | 3.41 |
| August | 3.98 | 0.391 | 24.23 | 3.48 |
| September | 4.09 | 0.421 | 24.7 | 3.07 |
| October | 4.55 | 0.509 | 25.28 | 2.56 |
| November | 4.95 | 0.519 | 25.85 | 2.08 |
| December | 5.17 | 0.526 | 25.35 | 2.09 |

2.2 Load Demand Model

The load demand for an appliance in an installation is given by Equation (1) [31]:

$$E = n_a P_{rating} \cdot t \quad (2)$$

Where, E is energy demand (kWh), n_a is number of such appliance, P_{rating} is power rating of the appliance (kW), t is duration of operating the appliance (hrs.).

Equation [3] is used to sum up energy demand of similar appliances such as lighting, and so on, [31]:

$$E_{total} = E_1 + E_2 + E_3 + E_4 + \dots + E_n \quad (3)$$

Also, the profile shows the energy demand over a 24-hour day, on which the energy system design is created. The load profile used in this work is based on the profile for industrial location obtained from HOMER. The input data to the simulation software and the design constraints are given in Tables 2 and 3 respectively.

Table 1 HOMER input data

| HOMER Constraints | Values |
|-----------------------------|--------|
| Discount rate, % | 6 |
| Inflation rate, % | 15.63 |
| Annual capacity shortage, % | 0% |
| Project life-span, yrs. | 25 |

Table 3 Design input specifications

| Design Components | Specifications |
|-------------------|--|
| Diesel generator | 6.6 kVA capacity |
| Solar PV | Canadian Solar MaxPower CS6X-325P |
| And another entry | Panel: flat plate Temp coefficient: 0.41 Operating temperature: 45 °C Technology: mono/poly crystalline De-rating factor: 0.88 Efficiency: 16.94%; Round trip efficiency is 80% |
| Storage | Battery – Crown 12CRV100 128kWh |
| Wind turbine | Generic 1kW |
| Converter | Generic System converter AC/DC |

2.3 Wind System Data, Sizing and Modeling

Wind systems thrive in huge climatic region or geographical locations. To know the wind potential of Oke-Imobi, the wind data was generated for the area. This wind data shows that July has the highest wind velocity while November has the least wind velocity.

If the range of the wind speed exceeds the cut-out speed, no power is created. The governing equations described by Equation (4) and (5) were applied using real-world experimental C_p figures from wind turbine datasheet. Equation (4) is applied for computational efficiency. The power output is the derivative of the wind turbine model. Equation (5) is a result of its implicit generality.

$$P = \begin{cases} 0 & 0 \leq v_u < v_{in} \\ \frac{1}{2} \rho A v_u^3 C_p & v_{in} \leq v_u \leq v_r \\ P_r & v_r \leq v_u < v_{out} \\ 0 & v_u \geq v_{out} \end{cases} \quad (4)$$

$$P = P_r \begin{cases} 0 & 0 \leq v_u < v_{in} \\ \frac{v_u - v_{in}}{v_r - v_{in}} & v_{in} \leq v_u \leq v_r \\ p_r & v_r \leq v_u < v_{out} \\ 0 & v_u \geq v_{out} \end{cases} \quad (5)$$

Where, P_r is the wind turbine's rated output rate power; v_u , is the actual wind speed corresponding to the tower height; v_{in} , is the wind turbine's cut-in speed, as determined by the turbine datasheet; v_r , is the turbine's rated speed as determined by the turbine datasheet; and v_{out} , is the turbine's cut-off/cut-out speed captured from the turbine datasheet.

2.4 Battery Sizing

Equation (6) is used to measure the battery's energy storage capacity [34]:

$$C_{BAh} = \frac{E_{db} \times AD}{DOD \times \eta_{BAh} \times V_B} \quad (6)$$

Where, C_{BAh} is total ampere-hour, E_{db} is battery energy required on daily basis, DOD is maximum battery discharge depth, η_{BAh} is round trip battery efficiency, and V_B is the nominal DC voltage of the battery block.

2.5 Inverter Sizing

Solar PV systems produce Direct Current (DC), which requires the use of an inverter to convert to Alternating Current (AC) to power the load. Sizing of the inverter is affected by the types of loads, either resistive or inductive loads [13]. Inverter's power rating can be calculated by Equation (7):

$$Inv_{size} = 3 \times (L_i) + L_{oth} \quad (7)$$

Where, Inv_{size} is the capacity of inverter in (kVA), L_i is the inductive load (kW), and L_{oth} is the other loads (kW).

2.6 Charge Regulator Sizing

To ensure charging the battery is done safely, correctly and adequately, the battery charging process has to be regulated. This also majorly helps to avoid over-charging. They are rated in maximum input voltage (V) and maximum charge current (A) [35]. As given by Equation (8), the charge regulated is exceeded by 30% to allow it to absorb any surge current coming from the array of the solar panel:

$$CR_{size} = 1.3 \times I_{sc} \quad (8)$$

Where, CR_{size} is the capacity of the solar charge controller and I_{sc} is the charge controller short-circuit current (A).

2.7 Solar PV Module Sizing

After the determination of the load requirement, the next stage is to determine the quantity of PV modules required for system reliability. In this step, the following are required to be put into consideration:

- Total daily power consumption = Total daily wattage of appliances.
- Total daily energy use = Total daily appliance usage in watt-hours.
- Total energy required from the panel = Total energy consumption per day $\times 1.3$, where 1.3 is the energy loss factor in the system. The minimal PV module required is given by Equation (9).

$$PV \text{ modules} = \frac{\text{Total appliance use in watt hours per day}}{\text{Total watt power of PV panel capacity needed} \times \text{number of PV panels needed}} \quad (9)$$

Constraints at the PV modules' terminals necessitate addition of extra parameters to the basic PV equation because modules are made up of numerous connected cells. The PV module (current) is given by Equation (10) [36]:

$$I = I_{pv} - I_0 \left(\exp \left(\frac{V + R_s I}{V_t \alpha} \right) - 1 \right) - \frac{V + R_s I}{R_p} \quad (10)$$

Where, I_{pv} is the photovoltaic current, I_0 saturation current, $V_t = KT/q$ is thermal voltage of modules connected in series, R_s and R_p being the equivalent series and parallel resistance respectively, and α is the short-circuit temperature coefficient.

The maximum current output of the solar panel at nominal temperature and solar radiation (at 25°C and 1000 W/m²) is represented by Equation (11):

$$I_{mpp} = I_{pv,n} - I_{0,n} \left(\exp \left(\frac{V_{mpp} + R_s I_{mpp}}{V_{t,n} a} \right) - 1 \right) - \frac{V_{mpp} + R_s I_{mpp}}{R_p} \quad (11)$$

Where, V_{mpp} is the maximum power point (MPP) voltage, while I_{mpp} is the current at MPP at the thermal voltage of the modules.

2.8 Economic Analysis

The Cost of Electricity (COE) of various power systems is calculated using Equation (12) as follows in [37], [4]:

$$COE = \frac{\text{Total annualised cost of the system} \left(\frac{\$}{yr} \right)}{\text{Total electricity supplied} \left(\frac{kW}{yr} \right)} \quad (12)$$

The total annualized cost is computed from in Equation (13):

$$C_{ann,tot} = C_{NPC} \cdot CRF \quad (13)$$

Where, C_{NPC} is the Net Present Cost (NPC) of a system, CRF is capital recovery factor given by Equation (14) [37], [4]:

$$CRF_{(i,N)} = \frac{i(i+1)^N}{(i+1)^N - 1} \quad (14)$$

Where, N is the number of years the project will last, and i is the annual interest rate.

The net present cost (or life cycle cost) of the component is obtained from the present installation and operation costs all over the project lifespan less the present income earned over the duration of the project.

3. Results and Analysis

3.1 Results of Simulation and Sensitivity Analysis

The results of the simulation were analysed based on the electrical production, unmet electricity, fuel summary and emissions for the distributed generation scenarios. The optimization procedure for the given sensitivity variables were repeated using HOMER. For the wind turbine, the turbine height was also used as a sensitivity variable input. The impacts of this variable on electrical production and unmet electricity were examined.

3.1.1 Results of Model 1

Model 1 consists of solar, wind and diesel generator design. A converter size of 3kW was used. This configuration was simulated to supply power to the load as shown in Fig 2 until 4. The Autonomy is 78.7hrs. The solar-wind-diesel generator design produced 6,319 kWh/yr, with an excess electricity of 1694 kWh/yr (26.8% of produced power). The unmet electric load and the capacity shortage are both 0 kWh/yr respectively.

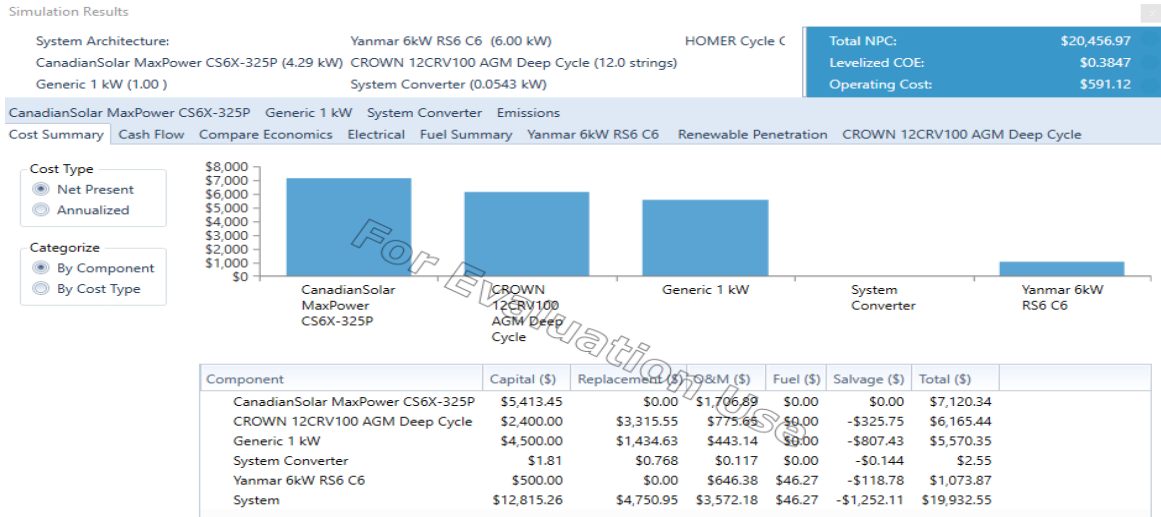


Fig. 2 Solar-wind-gas generator cost summary

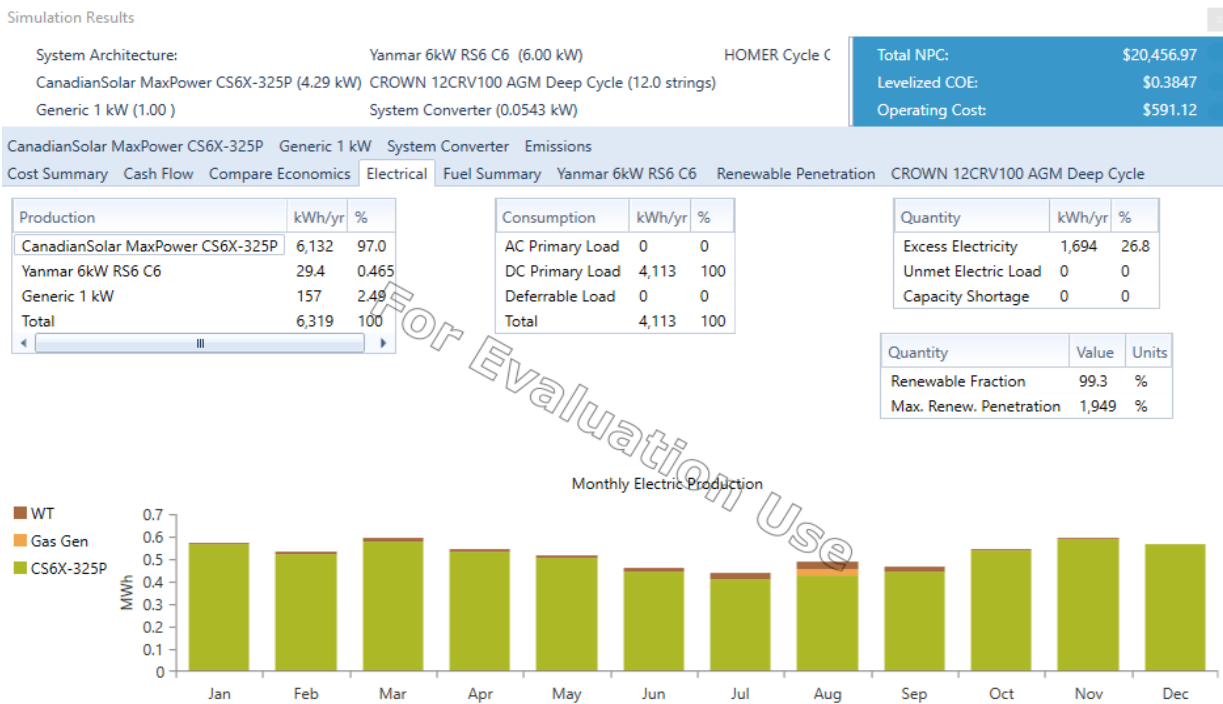


Fig. 3 Solar-wind-gas generator electrical result

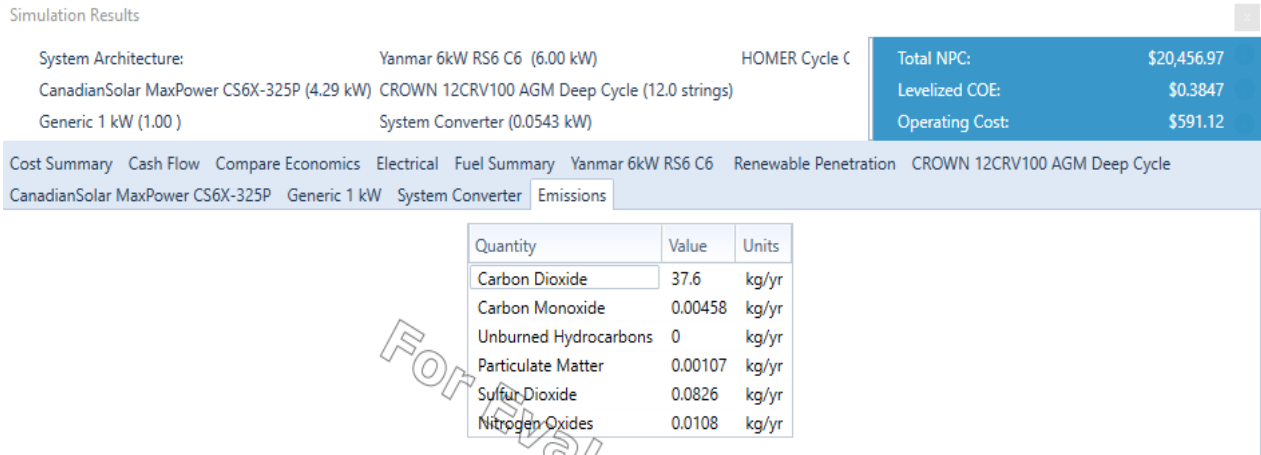


Fig. 4 Solar-wind-gas generator emission results

3.1.2 Results of Model 2

Model 2 consists of wind and diesel generator design. A converter size of 3kW was used. This configuration was simulated to supply power to the load as shown in Fig 5 until 7. The Autonomy is 177hrs. The wind-gas generator design produced 5,043 kWh/yr., with an excess electricity of 198 kWh/yr (3.92% of produced power). The Unmet Electric load and the Capacity Shortage are both 0 kWh/yr respectively.

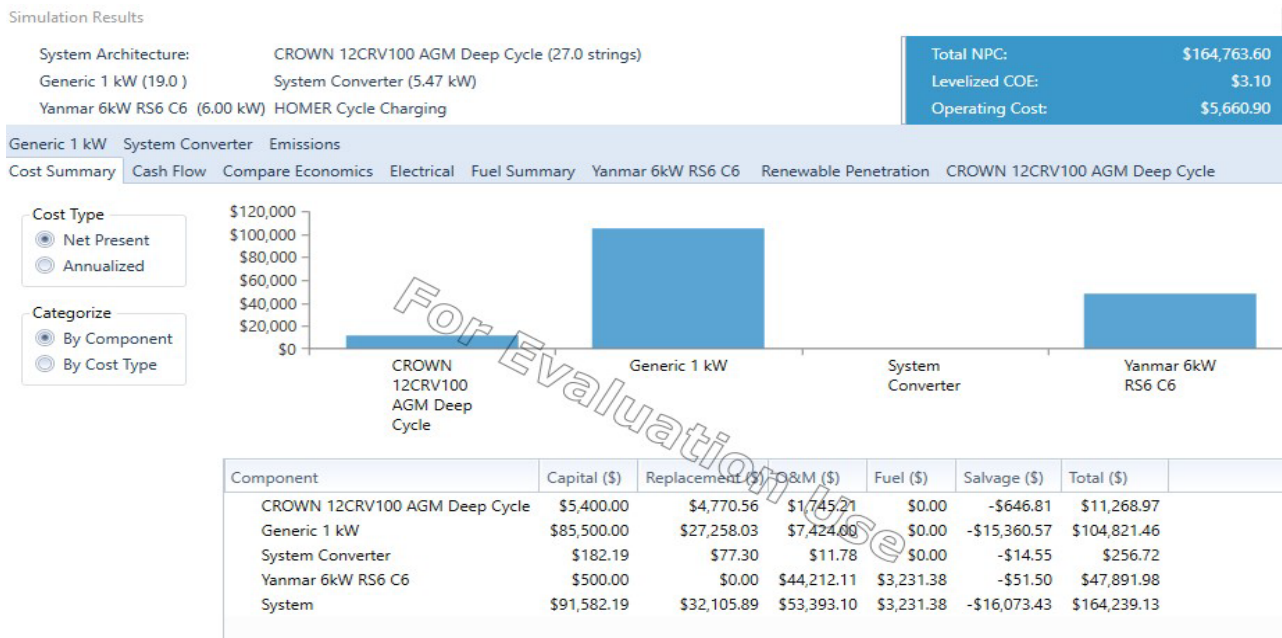


Fig. 5 Wind-gas generator cost summary

Simulation Results

System Architecture: CROWN 12CRV100 AGM Deep Cycle (27.0 strings)
 Generic 1 kW (19.0) System Converter (5.47 kW)
 Yanmar 6kW RS6 C6 (6.00 kW) HOMER Cycle Charging

Total NPC: \$164,763.60
 Levelized COE: \$3.10
 Operating Cost: \$5,660.90

Generic 1 kW System Converter Emissions
 Cost Summary Cash Flow Compare Economics Electrical Fuel Summary Yanmar 6kW RS6 C6 Renewable Penetration CROWN 12CRV100 AGM Deep Cycle

| Production | kWh/yr | % |
|-------------------|--------|------|
| Yanmar 6kW RS6 C6 | 2,053 | 40.7 |
| Generic 1 kW | 2,990 | 59.3 |
| Total | 5,043 | 100 |

| Consumption | kWh/yr | % |
|-----------------|--------|-----|
| AC Primary Load | 0 | 0 |
| DC Primary Load | 4,113 | 100 |
| Deferrable Load | 0 | 0 |
| Total | 4,113 | 100 |

| Quantity | kWh/yr | % |
|---------------------|--------|------|
| Excess Electricity | 198 | 3.92 |
| Unmet Electric Load | 0 | 0 |
| Capacity Shortage | 0 | 0 |

| Quantity | Value | Units |
|-------------------------|-------|-------|
| Renewable Fraction | 50.1 | % |
| Max. Renew. Penetration | 3,450 | % |

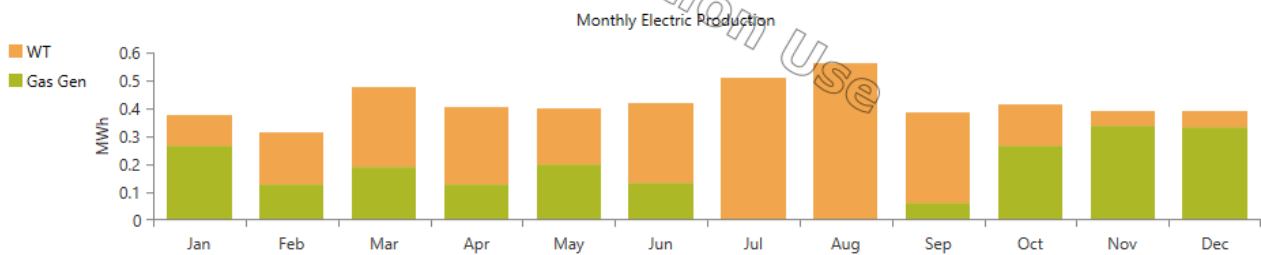


Fig. 6 Wind-gas generator electrical result

Simulation Results

System Architecture: CROWN 12CRV100 AGM Deep Cycle (27.0 strings)
 Generic 1 kW (19.0) System Converter (5.47 kW)
 Yanmar 6kW RS6 C6 (6.00 kW) HOMER Cycle Charging

Total NPC: \$164,763.60
 Levelized COE: \$3.10
 Operating Cost: \$5,660.90

Cost Summary Cash Flow Compare Economics Electrical Fuel Summary Yanmar 6kW RS6 C6 Renewable Penetration CROWN 12CRV100 AGM Deep Cycle
 Generic 1 kW System Converter Emissions

| Quantity | Value | Units |
|-----------------------|--------|-------|
| Carbon Dioxide | 2,627 | kg/yr |
| Carbon Monoxide | 0.320 | kg/yr |
| Unburned Hydrocarbons | 0 | kg/yr |
| Particulate Matter | 0.0750 | kg/yr |
| Sulfur Dioxide | 5.77 | kg/yr |
| Nitrogen Oxides | 0.755 | kg/yr |

Fig. 7 Wind-gas generator emission

3.1.3 Results of Model 3

Model 3 consists of solar-gas generator design. This configuration was simulated to supply power to the load as shown in Figure 8 until 10. A converter size of 3kW was used. The Autonomy is 85.3hrs. The solar-gas generator design produced 6,126 kWh/yr., with an excess electricity of 1526 kWh/yr (24.8% of produced power). The Unmet Electric load and the Capacity Shortage are both 0kWh/yr respectively.

Simulation Results

System Architecture: CROWN 12CRV100 AGM Deep Cycle (13.0 strings)
 CanadianSolar MaxPower CS6X-325P (4.29 kW) HOMER Cycle Charging
 Yanmar 6kW RS6 C6 (6.00 kW)

| | |
|-----------------|-------------|
| Total NPC: | \$14,596.51 |
| Levelized COE: | \$0.2745 |
| Operating Cost: | \$470.95 |

CanadianSolar MaxPower CS6X-325P Emissions

Cost Summary | Cash Flow | Compare Economics | Electrical | Fuel Summary | Yanmar 6kW RS6 C6 | Renewable Penetration | CROWN 12CRV100 AGM Deep Cycle

- Cost Type
- Net Present
 - Annualized
- Categorize
- By Component
 - By Cost Type

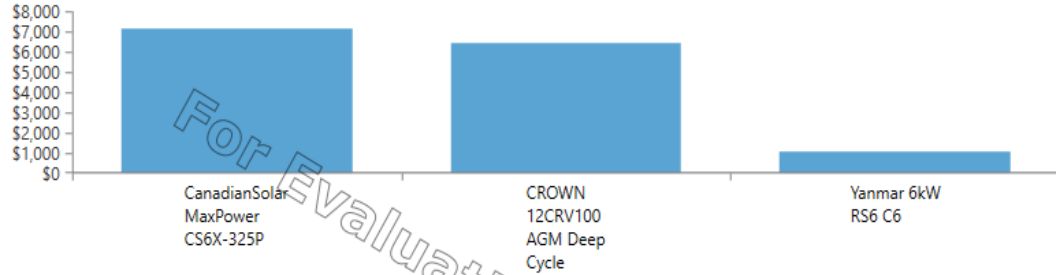


Fig. 8 Solar-gas generator cost summary

Simulation Results

System Architecture: CROWN 12CRV100 AGM Deep Cycle (13.0 strings)
 CanadianSolar MaxPower CS6X-325P (4.29 kW) HOMER Cycle Charging
 Yanmar 6kW RS6 C6 (6.00 kW)

| | |
|-----------------|-------------|
| Total NPC: | \$14,596.51 |
| Levelized COE: | \$0.2745 |
| Operating Cost: | \$470.95 |

CanadianSolar MaxPower CS6X-325P Emissions

Cost Summary | Cash Flow | Compare Economics | Electrical | Fuel Summary | Yanmar 6kW RS6 C6 | Renewable Penetration | CROWN 12CRV100 AGM Deep Cycle

| Production | kWh/yr | % |
|----------------------------------|--------|-------|
| CanadianSolar MaxPower CS6X-325P | 6,126 | 99.5 |
| Yanmar 6kW RS6 C6 | 31.8 | 0.516 |
| Total | 6,158 | 100 |

| Consumption | kWh/yr | % |
|-----------------|--------|-----|
| AC Primary Load | 0 | 0 |
| DC Primary Load | 4,113 | 100 |
| Deferrable Load | 0 | 0 |
| Total | 4,113 | 100 |

| Quantity | kWh/yr | % |
|---------------------|--------|------|
| Excess Electricity | 1,526 | 24.8 |
| Unmet Electric Load | 0 | 0 |
| Capacity Shortage | 0 | 0 |

| Quantity | Value | Units |
|-------------------------|-------|-------|
| Renewable Fraction | 99.2 | % |
| Max. Renew. Penetration | 1,943 | % |

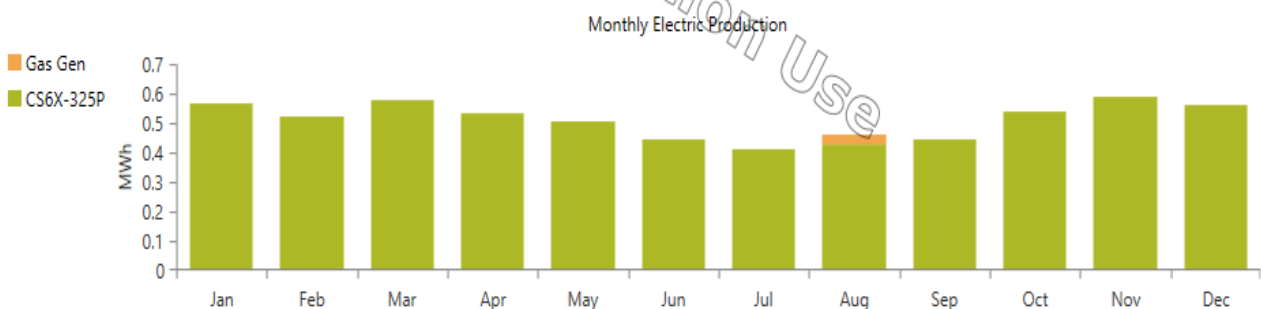


Fig. 9 Solar-gas generator electrical result

Simulation Results

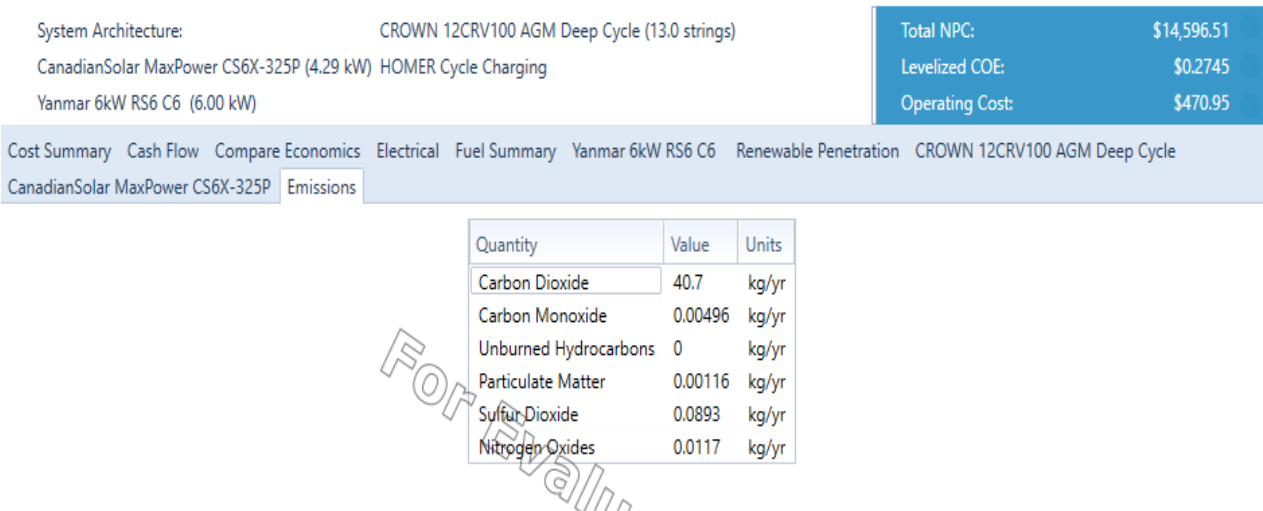


Fig. 10 Solar-gas generator emission

3.1.4 Results of Model 4

Model 4 consists of solar-wind design. A converter size of 3kW was used. This configuration was simulated to supply power to the load as shown in Figure 11 until 13. The Autonomy is 19.7hrs. The solar-wind design produced 4,509 kWh/yr., with an excess electricity of 632 kWh/yr (14.0% of produced power). The Unmet Electric load is 621 kWh/yr and the Capacity Shortage is 811 kWh/yr.

Simulation Results

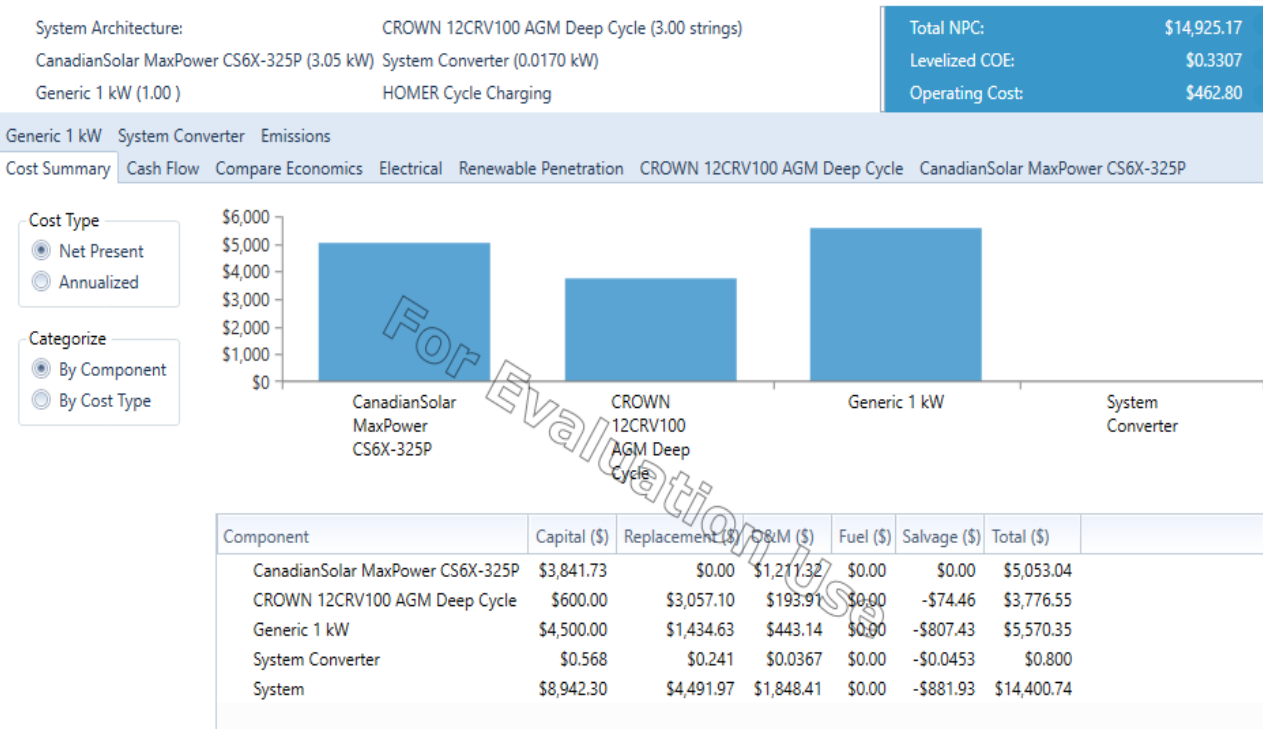


Fig. 11 Solar-wind cost summary

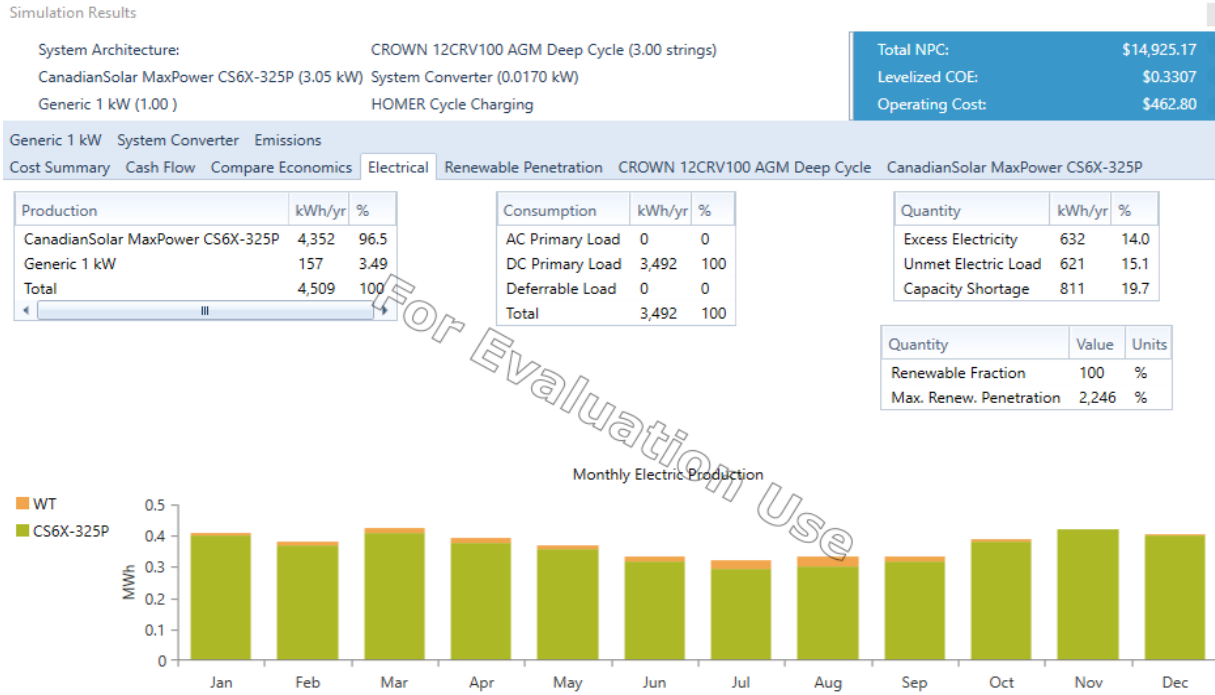


Fig. 12 Solar-wind electrical result

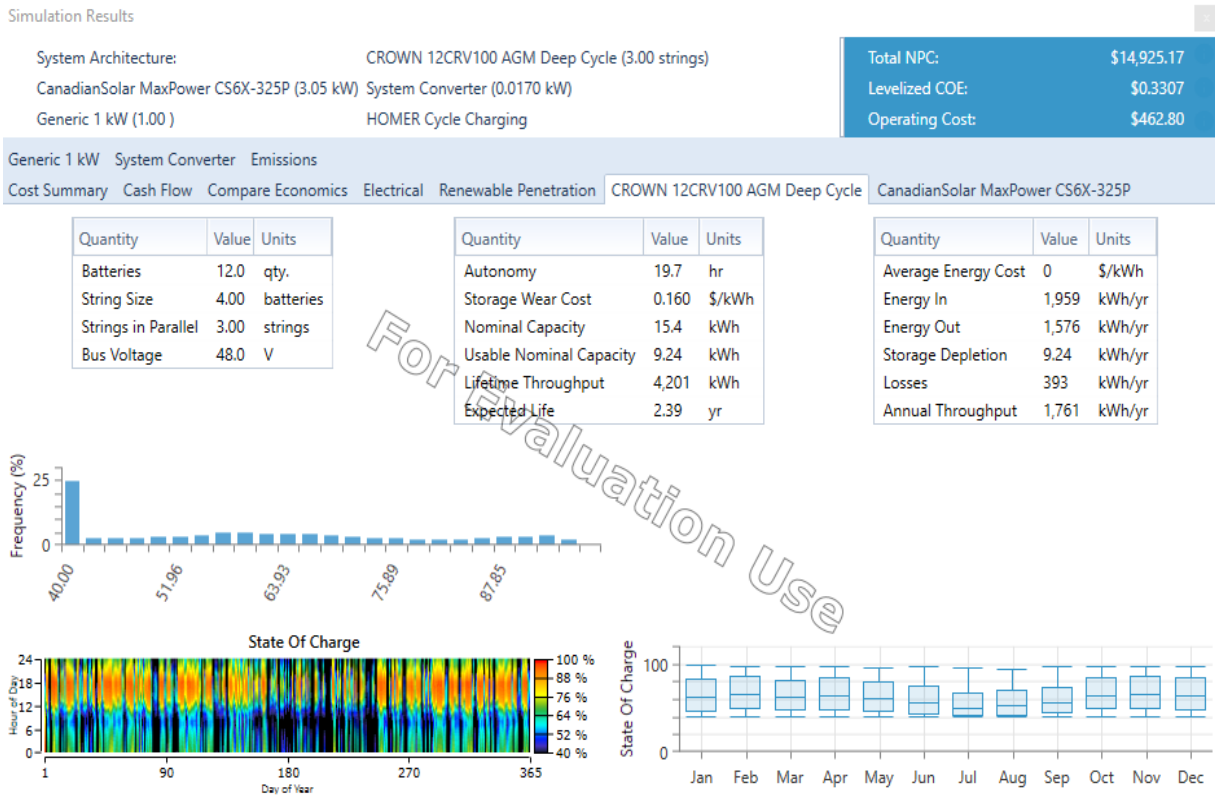


Fig. 13 Solar-wind battery result

Another simulation was performed by suggesting an increase in the PV capacity so as to investigate whether the unmet load will be reduced. A 28.8 kW PV capacity was then simulated with use of a 5kW converter size. The PV-based TCS produced 40,875 kWh/yr. with excess electricity of 8,838kWh/yr., Unmet Electric load of 3,258 kWh/yr. (10.6%) and Capacity Shortage of 4,626kWh/yr. (15.1%). The cost of Electricity (COE) is \$0.543/kWh.

3.2 Summary of Models Results

Table 4 shows the summary of the results obtained for the different models of energy resources mix. From the technical and economic perspectives, the results of Model 3 energy mix demonstrate optimal performance with lowest amount of excess power of 198kWh/yr. The excess power was more or less wasted power since there was no plan to sell excess power to anyone. The model also has the lowest Net Present Cost (NPC) of \$14,596.51, Cost of Electricity (COE) of \$0.2745/kWh and second lowest operating cost of \$470.95. This is actually because of the nature of the rural location, the wind current showed consistent availability and remarkable strength. So that this coupled with the generator supply, optimality is improved.

Table 4 Comparative analysis of results of energy mix models

| Energy Resources Model | Model 1: Solar, Wind and Generator | Model 2: Solar and Generator | Model 3: Wind and Generator | Model 4: Solar and Wind |
|----------------------------|--|------------------------------------|-----------------------------------|-------------------------------|
| Autonomy (Hours) | 78.4 | 85.3 | 177 | 19.7 |
| Power Produced (kWh/yr) | 6,319 | 6,126 | 5,043 | 4,509 |
| DC Primary Load (kWh/yr) | 4,113 | 4,113 | 4,113 | 3,492 |
| Excess (kWh/yr) | 1,694 | 1526 | 198 | 632 |
| %age Excess | 26.8 | 24.8 | 3.92 | 14 |
| Unmet Load (kWh/yr) | 0 | 0 | 0 | 621 |
| Capacity Shortage (kWh/yr) | 0 | 0 | 0 | 811 |
| Total NPC (\$) | 20,456.97 | 164,763.60 | 14,596.51 | 14,925.17 |
| Levelised COE (\$/kWh) | 0.3847 | 3.10 | 0.2745 | 0.3307 |
| Operating Cost (\$) | 591.12 | 5,660.90 | 470.95 | 462.80 |

From the emission perspective and the environmental implications of the different energy resources models, Table 5 presents data on the dangerous gas emissions form the different energy mix models.

Table 5 Dangerous gas emission of each model

| Energy Resources Model | Model 1: Solar, Wind and Generator | Model 2: Solar and Generator | Model 3: Wind and Generator | Model 4: Solar and Wind |
|------------------------------|--|------------------------------------|-----------------------------------|----------------------------|
| Carbon monoxide (kg/yr) | 0.00458 | 0.00496 | 0.320 | Zero Emission but suffer: |
| Unburned hydrocarbon (kg/yr) | 0 | 0 | 0 | Storage Wear Cost of |
| Particulate matters (kg/yr) | 0.00107 | 0.00116 | 0.0750 | 0.016 \$/kWh and |
| Sulfur dioxide (kg/yr) | 0.0826 | 0.893 | 5.77 | Storage Depletion of 9.24 |
| Nitrogen oxide (kg/yr) | 0.0108 | 0.0117 | 0.755 | kWh/yr |

From Table 5, Model 3 that proved optimal in technical and economic perspectives is worst from the perspective of emission of dangerous gases and particulate materials. Model 1 is least in emission from diesel generator because it depends least on the use of diesel generator apart from Model 4.

3.3 Summary of Models Results

Table 6 shows the summary of the results obtained for the different models of energy resources mix. From the technical and economic perspectives, the results of Model 3 energy mix demonstrate optimal performance with lowest amount of excess power of 198kWh/yr. The excess power was more or less wasted power since there was no plan to sell excess power to anyone. The Model also has the lowest Net Present Cost (NPC) of \$14,596.51, Cost of Electricity (COE) of \$0.2745/kWh and second lowest operating cost of \$470.95. This is actually because of the nature of the rural location, the wind current showed consistent availability and remarkable strength. So that this coupled with the generator supply, optimality is improved.

Table 6 Comparative analysis of results of energy mix models

| Energy Resources Model | Model 1: Solar, Wind and Generator | Model 2: Solar and Generator | Model 3: Wind and Generator | Model 4: Solar and Wind |
|----------------------------|--|------------------------------------|-----------------------------------|-------------------------------|
| Autonomy (Hours) | 78.4 | 85.3 | 177 | 19.7 |
| Power Produced (kWh/yr) | 6,319 | 6,126 | 5,043 | 4,509 |
| DC Primary Load (kWh/yr) | 4,113 | 4,113 | 4,113 | 3,492 |
| Excess (kWh/yr) | 1,694 | 1526 | 198 | 632 |
| %age Excess | 26.8 | 24.8 | 3.92 | 14 |
| Unmet Load (kWh/yr) | 0 | 0 | 0 | 621 |
| Capacity Shortage (kWh/yr) | 0 | 0 | 0 | 811 |
| Total NPC (\$) | 20,456.97 | 164,763.60 | 14,596.51 | 14,925.17 |
| Levelised COE (\$/kWh) | 0.3847 | 3.10 | 0.2745 | 0.3307 |
| Operating Cost (\$) | 591.12 | 5,660.90 | 470.95 | 462.80 |

From the emission perspective and the environmental implications of the different energy resources models, Table 7 presents data on the dangerous gas emissions from the different energy mix models.

Table 7 Dangerous gas emission of each model

| Energy Resources Model | Model 1: Solar, Wind and Generator | Model 2: Solar and Generator | Model 3: Wind and Generator | Model 4: Solar and Wind |
|------------------------------|--|------------------------------------|-----------------------------------|--|
| Carbon monoxide (kg/yr) | 0.00458 | 0.00496 | 0.320 | Zero Emission but suffer: Storage Wear Cost of 0.016 \$/kWh and Storage Depletion of 9.24 kWh/yr |
| Unburned hydrocarbon (kg/yr) | 0 | 0 | 0 | |
| Particulate matters (kg/yr) | 0.00107 | 0.00116 | 0.0750 | |
| Sulfur dioxide (kg/yr) | 0.0826 | 0.893 | 5.77 | |
| Nitrogen oxide (kg/yr) | 0.0108 | 0.0117 | 0.755 | |

From Table 6, Model 3 that proved optimal in technical and economic perspectives is worst from the perspective of emission of dangerous gases and particulate materials. Model 1 is least in emission from diesel generator because it depends least on the use of diesel generator apart from Model 4.

4. Conclusion

This work designed optimum hybrid power supply solution for remote off-grid TCS making a case study of the one at Oke-Imobi in Ogun State, Nigeria. It set out to analyse how solar, wind and diesel-fuelled generator can be used to meet the energy demand of TCS in remote locations. The three energy resources were combined with battery energy storage bank and the use of HOMER software simulation tool. Inputs were taken from technical, economic, and environmental factors, and used to obtain cost effective solutions. Simulations of mix of energy sources of solar-wind design, solar-diesel generator design, wind-diesel generator design, solar-wind-diesel generator design models were carried out. The yearly electricity production and unmet demand was used to ascertain the technical performance. Solar-wind design model for the TCS load is limited due to the intermittent characteristics of solar and wind energy which was augmented with the use of a diesel generator. PV/wind generation is the most feasible from technical, economic, and majorly environmental perspectives, but it has high unmet load and high-capacity shortage due to the variability in the availability of solar and wind resources all-year round. Therefore, there is the need to support it with minimal usage of diesel-fuelled generator, bringing us back to the choice of Model 1. This work becomes indispensable to research into bridging the electricity gap in remote communities to improve their socio-economic life through the use of mixed energy sources, particularly renewable energy resources, to drastically reduce emission of greenhouse gases from diesel fuel. In the future there is the need to introduce some other renewable energy sources like hydropower or biomass energy sources to address the variability in the availability of solar and wind sources, and thereby completely knock out the use of diesel-fuelled generator and the consequential emissions.

Acknowledgement

The authors declare that no funding was received from any organisation or funding body for this article.

Conflict of Interest

The authors declare that there is no conflict of interest whatsoever regarding the publication of this paper.

Author Contribution

The authors confirm contribution to the paper as follows: study conception and design: P.O. Obalisi, O. Ajayi; **data collection:** P.O. Obalisi, O. Ajayi; analysis and interpretation of results: P.O. Obalisi, O. Ajayi; **draft manuscript preparation:** P.O. Obalisi, O. Ajayi; All authors reviewed the results and approved the final version of the manuscript.

References

- [1] A. S. Sambo, B. Garba, I. H. Zarma and M. M. Gaji, "Electricity Generation and the Present Challenges in the Nigerian Power Sector," in 21st World Energy Congress (WEC) 2010, Montreal, Quebec, Canada, Sept. 2010, pp. 1-17.
- [2] P. Akanonu, "How big is Nigeria's power demand?," Energy for Growth Hub, Nov. 7, 2019. [Online]. Available: <https://www.energyforgrowth.org/memo/how-big-is-nigerias-power-demand/>.
- [3] E. I. Ohimain, "Can Nigeria Generate 30% of her Electricity from Coal by 2015," *International Journal of Energy and Power Engineering*, vol. 3, no. 1, pp. 28-37, Feb. 2014, doi: 10.11648/j.ijepe.20140301.15.
- [4] Y. S. Sanusi, H. A. Dandajeh, and H. Mustapha, "Techno-economic Analysis of Hybrid Diesel Generator/PV/Battery Power System for Telecommunication Application," *Journal of Science Technology and Education*, vol. 8, no. 3, pp. 77-91, Sept. 2020.
- [5] A. S. Aliyu, A. T. Ramli, and M. A. Saleh, "Nigeria Electricity Crisis: Power Generation Capacity Expansion and Environmental Ramifications," *Energy*, vol. 61, pp. 354-367, Nov. 2013, <https://doi.org/10.1016/j.energy.2013.09.011>.
- [6] O. M. Babatunde, I. H. Denwigwe, D. E. Babatunde, A. O. Ayeni, T. B. Adedjoja, and O. S. Adedjoja, "Techno-economic Assessment of Photovoltaic-Diesel Generator-Battery Energy System for Base Transceiver Stations Loads in Nigeria," *Cogent Engineering*, vol. 6, no. 1, pp. 1-19, Nov. 2019, <https://doi.org/10.1080/23311916.2019.1684805>.
- [7] L. Olatomiwa, S. Mekhilef, A. S. N. Huda, and K. Sanusi, "Techno-economic Analysis of Hybrid PV-diesel-battery and PV-wind-diesel-battery Power Systems for Mobile BTS: The Way Forward for Rural Development," *Energy Science and Engineering*, vol. 3, no. 4, pp. 271-285, April 2015, <https://doi.org/10.1002/ese3.71>.
- [8] B. Li, "Effective Energy Utilization Through Economic Development for Sustainable Management in Smart Cities," *Energy Reports*, vol. 8, pp. 4975-4987, April 2022, <https://doi.org/10.1016/j.egy.2022.02.303>.
- [9] O. W. Bello, J. F. Opadiji, N. Faruk, and Y. A. Adediran, "Opportunities for Universal Telecommunication Access in Rural Communities: A Case Research work of 15 Rural Villages in Nigeria's Kwara State," *The African Journal of Information and Communication (AJIC)*, vol. 17, pp. 139-163, Dec. 2016, <https://journals.co.za/doi/pdf/10.10520/EJC-7cbb4afc2>.
- [10] A. O. Acheampong, M. O. Erdiaw-Kwasie, and M. Abunyewah, "Does Energy Accessibility Improve Human Development? Evidence from Energy-Poor Regions," *Energy Economics*, vol. 96, 05165, April 2021, <https://doi.org/10.1016/j.eneco.2021.105165>.
- [11] B. Attigah, and L. Mayer-Tasch, "The Impact of Electricity Access on Economic Development - A Literature Review," in *Productive Use of Energy (PRODUSE): Measuring Impacts of Electrification on Micro-Enterprises in Sub-Saharan Africa*, Mayer-Tasch, L. and Mukherjee, M. and Reiche, K. (eds.), Eschborn, Germany:Deutsche Gesellschaft für Internationale Zusammenarbeit (GIZ) GmbH, 2013, pp. 1-26.
- [12] S. O. Oyedepo, "Energy and Sustainable Development in Nigeria: The Way Forward," *Energy, Sustainability and Society*, vol. 2, no. 1, pp. 1-17, Jul. 2012, <http://dx.doi.org/10.1186/2192-0567-2-15>.
- [13] W. S. Ebhota, and P. Y. Tabakov, "The Place of Small Hydropower Electrification Scheme in Socioeconomic Stimulation of Nigeria," *International Journal of Low-Carbon Technologies*, vol. 13, no. 4, pp. 311-319, Dec. 2019, <https://doi.org/10.1093/ijlct/cty038>.
- [14] M. A. Bhuiyan, Q. Zhang, V. Khare, A. Mikhaylov, G. Pinter, and X. Huang, "Renewable Energy Consumption and Economic Growth Nexus—A Systematic Literature Review," *Frontiers in Environmental Science*, vol. 10, 878394, April 2022, <https://doi.org/10.3389/fenvs.2022.878394>.
- [16] J. A. Salah. (2019). Basics of Solar PV System [Online]. Available: <http://dx.doi.org/10.13140/RG.2.2.10829.59363>.

- [17] G. Perkins, "Techno-Economic Comparison of The Levelized Cost of Electricity Generation from Solar PV and Battery Storage with Solar PV and Combustion of Bio-Crude Using Fast Pyrolysis of Biomass," *Energy Conversion and Management*, vol. 171, pp. 1573-1588, Sept. 2018, <https://doi.org/10.1016/j.enconman.2018.06.090>.
- [18] A. K. V. and A. Verma, "Optimal Techno-Economic Sizing of a Solar-Biomass-Battery Hybrid System for Off-Setting Dependency on Diesel Generators for Microgrid Facilities," *Journal of Energy Storage*, vol. 36, 102251, April 2021, <https://doi.org/10.1016/j.est.2021.102251>.
- [19] H. J. Wagner, "Introduction to Wind Energy Systems," *The European Physical Journal Conferences*, vol. 189, 00005, Jan. 2018, <http://dx.doi.org/10.1051/epjconf/201818900005>.
- [20] M. Zilberman. (2017). Optimization of Small, Low Cos, Vertical Axis Wind Turbine for Private and Institutional Use [Online]. Available: <http://dx.doi.org/10.13140/RG.2.2.15724.67202>.
- [21] B. I. Kunya, and A. Ahmed, "Performance Analysis of Two Different Sizes of Wind Turbine Rotors Based on Nigerian Low Wind Regime.," *Nigerian Journal of Technology (NIJOTECH)*, vol. 41, no. 1, pp. 77–82, Jan. 2022, <http://dx.doi.org/10.4314/njt.v41i1.11>.
- [22] G. P. Hammond, and T. Hazeldine, "Indicative Energy Technology Assessment Of Advanced Rechargeable Batteries," *Applied Energy*, vol. 138, pp. 559-571, Jan. 2015, <https://doi.org/10.1016/j.apenergy.2014.10.037>.
- [23] A. Aluko, and A. Knight, A. (2023). "A Review on VRFB Storage Systems for Large-Scale Power Systems Application," in *IEEE Access*, vol. 11, pp. 13773-13793, Feb. 2023, <https://doi.org/10.1109/ACCESS.2023.3243800>.
- [24] H. Wanga, S. A. Pourmousavia, W. L. Soong, X. Zhang, and N. Ertugrul, "Battery and Energy Management System for Vanadium Redox Flow Battery: A Critical Review and Recommendations," *Journal of Energy Storage*, vol. 58, 106384, Feb. 2023, <https://doi.org/10.1016/j.est.2022.106384>.
- [25] J. Xu, X. Cai, S. Cai, Y. Shao, C. Hu, S. Lu, and S. Ding, "High-Energy Lithium-Ion Batteries: Recent Progress and a Promising Future in Applications," *Energy and Environment Materials*, vol. 6, no. 5, e12450, June 2022, <https://doi.org/10.1002/eem2.12450>.
- [26] S. Chen, Z. Wang, M. Zhang, X. Shi, L. Wang, W. An, Z. Li, F. Pan, and L. Yang, "Practical Evaluation of Prelithiation Strategies for Next-Generation Lithium-Ion Batteries," *Carbon Energy*, vol. 5, no. 8, e323, Mar. 2023, <https://doi.org/10.1002/cey2.323>.
- [27] L. Zhao, T. Zhang, W. Li, T. Li, L. Zhang, X. Zhang, and Z. Wang, "Engineering of Sodium-Ion Batteries: Opportunities and Challenges," *Engineering*, vol. 24, pp. 172–183, May 2023, <http://doi.org/10.1016/j.eng.2021.08.032>.
- [28] Y. S. Mohammed, M. W. Mustafa, N. Bashir, and A. S. Mokhtar, "Renewable energy re- sources for distributed power generation in Nigeria: a review of the potential," *Renewable and Sustainable Energy Reviews*, vol. 22, pp. 257-68, June 2013, <https://doi.org/10.1016/j.rser.2013.01.020>.
- [29] F. Odoi-Yorke, and A. Woenagnon, "Techno-Economic Assessment of Solar PV/Fuel Cell Hybrid Power System for Telecom Base Stations in Ghana," *Cogent Engineering*, vol. 8, no. 1, Mar. 2021, <https://doi.org/10.1080/23311916.2021.1911285>
- [30] Solargis. Accessed: May 30, 2025. [Online] Available: <https://solargis.info/>.
- [31] National Aeronautics and Space Administration (NASA) Prediction of worldwide POWER solar energy resource data. Accessed: Oct. 5, 2022. [Online]. Available: <https://power.larc.nasa.gov/docs/services/api/temporal/monthly/>.
- [32] S. Yashwant, S. C. Gupta, and A. K. Bohre, "Review of hybrid renewable energy systems with comparative analysis of off-grid hybrid system," *Renewable and Sustainable Energy Reviews*, vol. 81, pp. 2217-2235, Jan. 2018, <https://doi.org/10.1016/j.rser.2017.06.033>.
- [33] P. Gildert. (2006). Power System Efficiency in Wireless Communication [Online]. Available: https://www.thierry-lequeu.fr/data/APEC/2006/APEC_2006_SP2_1.pdf.
- [34] A. Ayang, S. Ngohe-Ekam, B. Videme, and J. Temga, "Power Consumption: Base Stations of Telecommunication in Sahel Zone of Cameroon: Typology Based on the Power Consumption—Model and Energy Savings," *Journal of Energy*, vol. 2016, no. 1, 3161060, Jul. 2016, <http://dx.doi.org/10.1155/2016/3161060>.
- [35] I. A. Ibrahim, T. Khatib, and A. Mohamed, "Optimal Sizing of a Standalone Photovoltaic System for Remote Housing Electrification Using Numerical Algorithm and Improved System Models," *Energy*, vol. 126, pp. 392-403, May 2017, <https://doi.org/10.1016/j.energy.2017.03.053>.

- [36] P. Malik, M. Awasthi, and S. Sinha, "Study on an Existing PV/Wind Hybrid System Using Biomass Gasifier for Energy Generation," *Pollution*, vol. 6, no. 2, pp. 325-336, Feb. 2020, <https://doi.org/10.22059/poll.2020.293034.719>.
- [37] E. M. Salilih, and Y. T. Birhane, "Modeling and Analysis of Photo-Voltaic Solar Panel under Constant Electric Load," *Journal of Renewable Energy*, vol. 2019, no. 1, 9639480, Aug. 2019, <https://doi.org/10.1155/2019/9639480>.
- [38] Y. S. Sanusi, E. M. A. Mokheimer, and M. A. Habib, "Thermo-Economic Analysis of Integrated Membrane-SMR ITM-Oxy-Combustion Hydrogen and Power Production Plant," *Applied Energy*, vol. 204, pp. 626-640, Oct. 2017, <https://doi.org/10.1016/j.apenergy.2017.07.020>.